ARMY RESEARCH LABORATORY

Viscoelastic Response of Prestressed Composite Cylinders for Rotating Machinery Applications

by Jerome T. Tzeng

ARL-TR-1590

January 1998

19980206 064

DTIC QUALITY INSPECTED 2

Army Research Laboratory

Aberdeen Proving Ground, MD 21005-5066

Viscoelastic Response of Prestressed Composite Cylinders for Rotating Machinery Applications

Jerome T. Tzeng
Weapons and Materials Research Directorate, ARL

Abstract

Energy storage devices such as composite rotors are built with radial precompression to enhance mechanical performance; however, the preload might decrease due to the viscoelastic behavior of materials at elevated temperatures. In this investigation, an analytical solution is developed to study the viscoelastic problem of thick-walled cylinders. The analysis accounts for ply-by-ply variations of properties, fiber orientations, and temperature gradients through the thickness of cylinders. Fiber-reinforced composite materials generally illustrate extreme anisotropy in viscoelastic behavior. The viscoelasticity exists mainly in matrix-dominant properties such as transverse and shear while the fiber-dominant properties behave more like elastic mediums. Accordingly, the viscoelastic characteristics of composite cylinders are quite different from those of isotropic cylinders. Currently, finite-element packages such as ABAQUS, ANSYS, and DYNA3D are not suitable for the viscoelastic analysis of composite cylinders because of the lack of anisotropic viscoelastic elements. The prestress in the hoop-wound fibers, which generates radial compression in the cylinders, might decrease due to Poisson's effect alone from the creep behavior in the transverse properties of composite. The result also shows the effects of layup construction and fiber orientations on the anisotropic behavior of composite cylinders.

Acknowledgment

INTENTIONALLY LEFT BLANK.

Table of Contents

INTENTIONALLY LEFT BLANK.

List of Figures

INTENTIONALLY LEFT BLANK.

1. Introduction

Composite materials are currently used for highly efficient rotors, as an energy storage device. For these applications, prestresses are built in during fabrication of the cylinders through a press-fit procedure to enhance the mechanical performance. In a high-speed rotor, centrifugal force resulting from the rotation during operation generates tensile stresses in the radial and circumferential directions. Since the composite rotors are primarily reinforced in a circumferential direction, the radial tensile is critical to the ultimate performance of the rotors due to the weakness of radial strength. Accordingly, it is crucial to build and maintain a certain level of radial compression in the rotor prior to operation. Reinforced composite materials are also used for construction of lightweight gun barrels. Composite gun tubes are generally built with a metal liner and a composite overwrap. Because of a thick-walled construction, there is a stress gradient through the thickness of barrels as subjected to propellant pressure. For a gun barrel application, there is a stress gradient through the wall thickness. The stress gradient has to be minimized to achieve the optimal structural performance. Composite gun barrels must be prestressed; therefore, the composite overwrap is in a state of tension to induce compression in the steel liner.

Polymer materials in general behave viscoelastically, which means that creep associated with stress relaxation occurs in a long period of time, especially at elevated temperatures (Ferry 1961). The associated stress relaxation in the composite wall results in loss of the prestresses and potentially leads to structural failures or downgrade in performance. Fiber-reinforced composites with polymer matrix carry the same characteristic, but behave more complicatedly due to anisotropy. For carbon-fiber composite, fiber-dominant properties such as modulus in the fiber direction are sort of elastic. The viscoelasticity exists mainly in matrix-dominant properties such as transverse moduli and shear properties. Because of the extreme anisotropic characteristic, a composite cylinder will behave quite differently from one built with isotropic materials. The objective of this investigation is to develop an analytical method to study the viscoelastic behavior of the thick-walled composite cylinders. The analysis can be applied to the design of flywheel machinery and overwrapped composite gun tubes.

1

To date, activities in the research of viscoelasticity have mainly concerned isotropic materials included in the studies by Muki and Sternberg (1961), Schapery (1964), Williams (1964), and Christensen (1982). These basic theories of viscoelasticity were then extended to the area of heterogeneous and anisotropic materials for a variety of applications. Hashin (1965) used the effective relaxation moduli and creep compliances to define the macroscopic viscoelastic behavior of linear viscoelastic heterogeneous media and its implementation in viscoelastic modeling. The general formulation of linear viscoelastic boundary value problems of composite materials, including the thermal viscoelastic problems for thermorheologically simple materials and the applications of the correspondence principle, were examined by Schapery (1967). Rogers and Lee (1964) investigated the viscoelastic behavior of an isotropic cylinder.

In the following research, the linear quasi-static viscoelastic behavior of a thick laminated composite cylinder with an elevated temperature change is studied. The analysis accounts for ply-by-ply variation of properties, temperature changes, and fiber orientations. The thick cylinder is assumed to be in the absence of thermomechanical coupling and to be in the state of generalized plane strain, such that all the stress and strain components are independent of the axial coordinate (Tzeng and Chien 1994). Moreover, due to the nature of axisymmetry, all the stress and strain components are also independent of the circumferential coordinate. The mechanical responses of this thick composite cylinder will, therefore, only have to satisfy the governing equation in the radial direction. Invoking the Boltzmann superposition integral for the complete spectrum of increments of anisotropic material constants with respect to time, the thermoviscoelastic constitutive relations of the anisotropic composite cylinder can be derived in integral forms. Since the thick composite cylinder is subjected to a constant elevated temperature change, and boundary conditions are all independent of time, formulations of the linear thermal viscoelastic problem can have forms identical to those of the corresponding linear thermoelastic problem by taking advantage of the elastic-viscoelastic correspondence principle. In other words, all of these integral constitutive equations reduce to algebraic relations that are very similar to those developed for thermoelastic media when they are Laplace transformed by means of the rule for convolution integrals. The thermoelastic analysis can thus be used to derive the transformed thermal viscoelastic solutions in the frequency domain.

2

2. Viscoelastic Formulation

Consider a filament-wound axisymmetric thick composite cylinder consisting of N layers with the axial coordinate z, the radial coordinate r, and the circumferential coordinate θ, as shown in Figure 1. This composite cylinder has the inner radius a, the outer radius b, and the length L. The Boltzmann superposition integral of a stress σ_{ij} (i, j = 1, 2, 3) and strain ϵ_{ij} (i, j = 1, 2, 3) relation for an isothermal viscoelastic problem with a constant temperature increase ΔT and the thermal expansion coefficient α_{kl} is

$$\sigma_{ij}(t) = \int_0^t C_{ij}^{kl}(T, t - \tau)\, \frac{\partial \epsilon_{kl}(\tau)}{\partial \tau} d\tau \; - \; \beta_{ij}(T, t) \Delta T \; , \tag{1}$$

where $C_{ij}^{kl}(T, t)$ is the relaxation modulus dependent on temperature T and time t,

$$C_{ij}^{kl}(T(t), t) = C_{ij}^{kl}(T_0, \lambda(t))$$

$$\lambda(t) = \frac{t}{a_T(T(t))} \; .$$

Here, T_0 is the base temperature, and a_T is the temperature-shift factor. $\beta_{ij}(T, t)$ is given by $B_{ij}(T, t) = C_{ij}^{kl}(T, t) \cdot \alpha_{kl}$. It is often desirable to use the inverse form of the constitutive relation (1),

$$\epsilon_{ij}(t) = \int_0^t A_{ij}^{kl}(T, t - \tau) \frac{\partial \sigma_{kl}(\tau)}{\partial \tau} d\tau \; + \; \psi_{ij}(T, t) \Delta T \; , \tag{2}$$

where $\psi_{ij}(T, t)$ is the tensor product of the creep compliance $A_{ij}^{kl}(T, t)$ and the thermal creep coefficient ϕ_{kl}. Since the elevated temperature change ΔT is constant above some reference value in time, the relaxation moduli and creep compliances are evaluated at that reference temperature regardless of whether or not the material is thermorheologically simple by employing the temperature-shift factor.
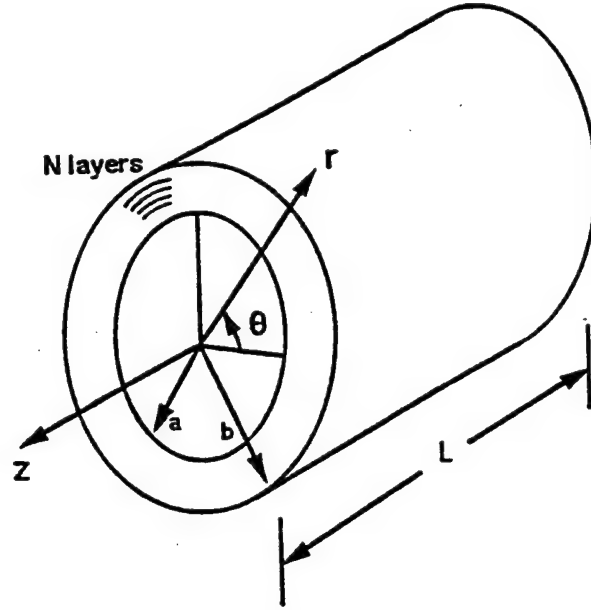
3

Figure 1. Continuity Cylindrical Coordinate System (r, q, z) of a Laminated Cylinder Containing N Layers.

The Laplace transform of a function f(t) is defined as

$$\bar{f} = \bar{f}(s) = \int_0^\infty e^{-st} f(t) \, dt, \tag{3}$$

where s is the Laplace transform variable. Applying (3) with the convolution rule to (1) and (2) reduces the integral constitutive equations to the following algebraic relations:

$$\bar{\sigma}_{ij} = \tilde{C}_{ij}^{kl} \, \tilde{\epsilon}_{kl} - \tilde{\beta}_{ij} \frac{\Delta T}{s}, \tag{4}$$

and the inverse form

$$\tilde{\epsilon}_{ij} = \tilde{A}_{ij}^{kl} \, \bar{\sigma}_{ij} + \tilde{\psi}_{ij} \frac{\Delta T}{s}, \tag{5}$$

respectively, where

$$\tilde{C}_{ij}^{kl} = s\bar{C}_{ij}^{kl}, \; \tilde{A}_{ij}^{kl} = s\bar{A}_{ij}^{kl}, \; \tilde{\alpha}_{ij} = s\bar{\alpha}_{ij}, \tilde{\phi}_{ij} = s\bar{\phi}_{ij}, \tilde{\beta}_{kl} = \tilde{C}_{ij}^{kl} \cdot \tilde{\alpha}_{ij}, \text{ and } \tilde{\psi}_{kl} = \tilde{A}_{ij}^{kl} \cdot \tilde{\phi}_{ij}.$$

Furthermore, it can be shown that $\left[\tilde{A}_{ij}^{kl}\right] = \left[\tilde{C}_{ij}^{kl}\right]^{-1}$.

4

Consider a corresponding thermoelastic problem with the transformed displacement components $\bar{u}$, $\bar{v}$, and $\bar{w}$ in the axial direction, the circumferential direction, and the radial direction, respectively, in each layer. The axisymmetric character of the thick composite cylinder along with the assumption of the state of generalized plane strain leads to a simplified displacement field, which reflects the circumferential independence and only-radial dependence of $\bar{w}$,

$$\bar{u}(r,\theta,z) = \bar{u}(r,z)$$
$$\bar{v}(r,\theta,z) = \bar{v}(r,z)$$
$$\bar{w}(r,\theta,z) = \bar{w}(r). \tag{6}$$

Substituting these transformed displacement components into the strain-displacement relations and invoking the compatibility conditions, one can derive explicit forms of $\bar{u}$ and $\bar{v}$. Since each layer of the thick laminated cylinder is cylindrically monoclinic in reference to the global coordinates, there is no coupling between transverse shears and other deformations. Accordingly, the vanishing shear traction boundary conditions and interface continuity conditions generate zero out-of-plane shear tractions and shear strains for each layer. Moreover, owing to the absence of torsional deformation, the transformed displacement components $\bar{u}$ and $\bar{v}$ become

$$\bar{u} = \bar{\epsilon}^0 z$$
$$\bar{v} = 0, \tag{7}$$

where the constant quantity $\bar{\epsilon}^0$ has the physical interpretation of transformed axial strain of a layer. In fact, $\bar{\epsilon}^0$, according to the present formulation, also represents the transformed axial strain of the entire composite cylinder. The calculation of $\bar{\epsilon}^0$ requires the knowledge of end boundary conditions and will be given later. Likewise, solving for $\bar{w}(r)$ requires the information of transformed strain components, the constitutive equations, as well as the equilibrium equations.

The previously transformed displacement field gives the transformed strain components in cylindrical coordinates

5

$$\bar{\epsilon}_{rr} = \frac{d\bar{w}(r)}{dr}$$

$$\bar{\epsilon}_{\theta\theta} = \frac{\bar{w}(r)}{r}$$

$$\bar{\epsilon}_{zz} = \frac{d\bar{u}}{dz} = \bar{\epsilon}^0$$

$$\bar{\epsilon}_{\theta r} = \bar{\epsilon}_{zr} = \bar{\epsilon}_z = 0 . \tag{8}$$

The unabridged form of the constitutive equation (4) for each layer in cylindrical coordinates with the radial coordinate r normal to the plane of symmetry is expressed as

$$
\begin{Bmatrix} \bar{\sigma}_{zz} \\ \bar{\sigma}_{\theta\theta} \\ \bar{\sigma}_{rr} \\ \bar{\sigma}_{\theta r} \\ \bar{\sigma}_{zr} \\ \bar{\sigma}_{z\theta} \end{Bmatrix} = \begin{bmatrix} \tilde{C}_{11} & \tilde{C}_{12} & \tilde{C}_{13} & 0 & 0 & \tilde{C}_{16} \\ \tilde{C}_{12} & \tilde{C}_{22} & \tilde{C}_{23} & 0 & 0 & \tilde{C}_{26} \\ \tilde{C}_{13} & \tilde{C}_{23} & \tilde{C}_{33} & 0 & 0 & \tilde{C}_{36} \\ 0 & 0 & 0 & \tilde{C}_{44} & \tilde{C}_{45} & 0 \\ 0 & 0 & 0 & \tilde{C}_{45} & \tilde{C}_{55} & 0 \\ \tilde{C}_{16} & \tilde{C}_{26} & \tilde{C}_{36} & 0 & 0 & \tilde{C}_{66} \end{bmatrix} \begin{Bmatrix} \bar{\epsilon}_{zz} \\ \bar{\epsilon}_{\theta\theta} \\ \bar{\epsilon}_{rr} \\ \bar{\epsilon}_{\theta r} \\ \bar{\epsilon}_{zr} \\ \bar{\epsilon}_{z\theta} \end{Bmatrix} - \frac{\Delta T}{s} \begin{Bmatrix} \tilde{B}_{zz} \\ \tilde{B}_{\theta\theta} \\ \tilde{B}_{rr} \\ 0 \\ 0 \\ \tilde{B}_{z\theta} \end{Bmatrix} . \tag{9}
$$

Furthermore, from the previous discussions, it can be shown that two of the three equilibrium equations are satisfied automatically. The only nontrivial equilibrium equation is the one in the radial direction:

$$\frac{\partial \bar{\sigma}_{rr}}{\partial r} + \frac{\bar{\sigma}_{rr} - \bar{\sigma}_{\theta\theta}}{r} = 0 . \tag{10}$$

Substituting (6), (7), and (8) into (9), the transformed stress components $\bar{\sigma}_{rr}$ and $\bar{\sigma}_{\theta\theta}$ are obtained in terms of the transformed radial displacement $\bar{w}$. Incorporating the resulting $\bar{\sigma}_{rr}$ and $\bar{\sigma}_{\theta\theta}$ functions with (10) gives a nonhomogeneous Euler differential equation of $\bar{w}$ for a layer

$$r^2 \frac{d^2\bar{w}}{dr^2} + r\frac{d\bar{w}}{dr} - \tilde{\lambda}^2\bar{w} = \frac{r}{\tilde{C}_{33}}\left[\frac{\Delta T}{s}(\tilde{B}_{rr} - \tilde{B}_{\theta\theta}) - (\tilde{C}_{13} - \tilde{C}_{12})\bar{\epsilon}^0 \right], \tag{11}$$

where

$$\tilde{\lambda}^2 = \frac{\tilde{C}_{22}}{\tilde{C}_{33}} . \tag{12}$$

Solving (11) for $\bar{w}$ yields

$$\bar{w} = \bar{A}_1 r^{\tilde{\lambda}} + \bar{A}_2 r^{-\tilde{\lambda}} + \tilde{w}_p , \tag{13}$$

where

$$\tilde{w}_p = \tilde{f}_1 \bar{\epsilon}^\circ r + \tilde{f}_3 r$$

$$\tilde{f}_1 = \frac{\tilde{C}_{12} - \tilde{C}_{13}}{\tilde{C}_{33} - \tilde{C}_{22}}$$

$$\tilde{f}_3 = \frac{\tilde{S}}{\tilde{C}_{33} - C_{22}}$$

$$\tilde{S} = \frac{\Delta T}{s} [\tilde{B}_{rr} - \tilde{B}_{\theta\theta}], \tag{14}$$

and $\bar{A}_1$ and $\bar{A}_2$ are coefficients to be determined from boundary and continuity conditions.

Finally, it is understood that the initial condition of the original thermoviscoelastic problem is displacement-free state of rest. The boundary conditions are of free tractions and, hence, of free transformed tractions on both inner and outer circular surfaces:

$$\bar{\sigma}_{rr} = \bar{\sigma}_{\theta r} = \bar{\sigma}_{zr} = 0 \quad \text{at} \quad r = a, b . \tag{15}$$

On both end surfaces, stress resultants are zero:

$$\sum_{k=1}^{N} \int_{r_i}^{r_o} \bar{\sigma}_{zz} r \, dr = \bar{\sigma}_{zr} = \bar{\sigma}_{z\theta} = 0 \quad \text{at} \quad z = 0, L , \tag{16}$$

7

where r_i and r_o are inner and outer radii, respectively, of the kth layer. The continuity conditions at each interface between two adjacent layers require continuous radial traction and continuous radial displacement at any instant as shown in Figure 2. Thus, when written in the transformed form, they become

$$\bar{\sigma}_{rr,o}^{(k)} - \bar{\sigma}_{rr,i}^{(k+1)} = 0 \tag{17}$$

and

$$\bar{w}_{,o}^{(k)} = \bar{w}_{,i}^{(k+1)}, \tag{18}$$

where $k = 1, \cdots, N - 1$, and subscripts i and o denote inner and outer surfaces, respectively.

Accordingly, the formulation accounts for ply-by-ply variations of material properties and temperature change. The matrix form numerical solution procedure with parallel computing techniques resolved the complexity and time-consuming calculation procedures in a Laplace transform of a multilayered composite cylinder (Chien and Tzeng 1995).
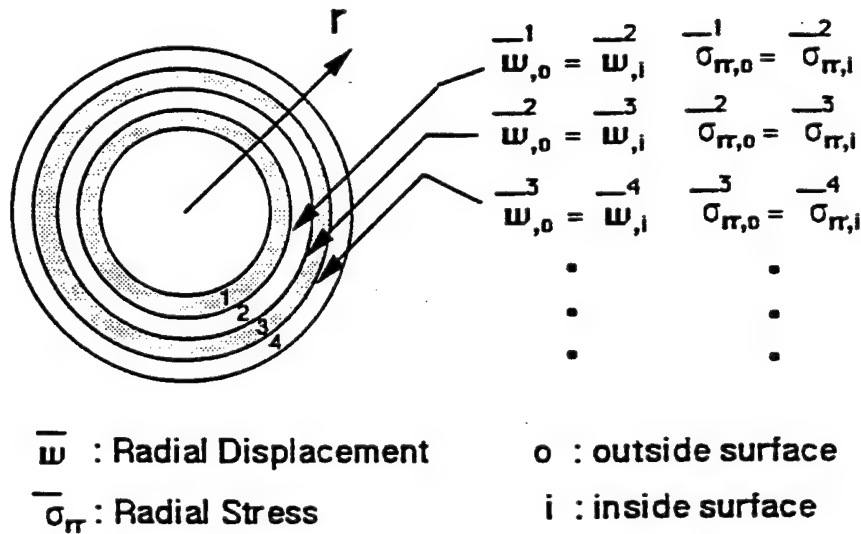

$$\bar{w}_{,o}^1 = \bar{w}_{,i}^2 \qquad \bar{\sigma}_{rr,o}^1 = \bar{\sigma}_{rr,i}^2$$

$$\bar{w}_{,o}^2 = \bar{w}_{,i}^3 \qquad \bar{\sigma}_{rr,o}^2 = \bar{\sigma}_{rr,i}^3$$

$$\bar{w}_{,o}^3 = \bar{w}_{,i}^4 \qquad \bar{\sigma}_{rr,o}^3 = \bar{\sigma}_{rr,i}^4$$

$\bar{w}$: Radial Displacement   o : outside surface

$\bar{\sigma}_{rr}$: Radial Stress   i : inside surface

Figure 2. Continuity Boundary Conditions of Radial Displacement and Stresses at the Interfaces of Adjacent Layers.

8

3. Relaxation of Thermal Stresses

The time-dependent thermal viscoelastic behavior of a 100-layer AS-4/3502 graphite epoxy composite cylinder subjected to a temperature increase $\Delta T = 150°$ C is examined. The composite cylinder has an inner radius a = 3.5 in, an outer radius b = 4.1 in, and a thickness of each layer $h = 6.0 \cdot 10^{-3}$ in. Stacking sequence is given as $[0/30/60/90]_{25}$ from inside out with the $0°$ direction coinciding with the axis of the cylinder. The creep properties of AS-4/3502 graphite epoxy and AS-4/PEEK thermoplastic laminate with a fiber volume fraction of 0.67 were investigated at different temperatures by Kim and Hartness (1987). Figure 3 shows the transverse and shear compliance of the composite at various temperatures. Increase of compliance with time due to creep behaviors of material was found at elevated temperatures.
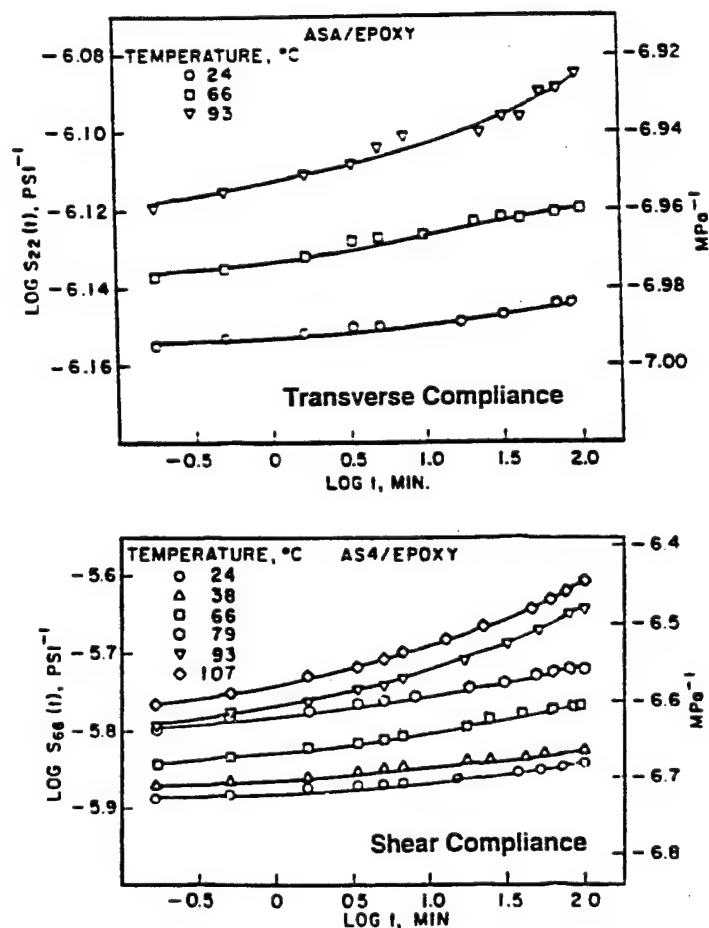

Figure 3. Time-Dependent Transverse and Shear Compliances at Various Temperatures (Kim and Hartness 1987).

9

In this study, the least-squares curve fitting was used to express the creep compliances from the original AS-4/3502 data at $T = 150°$ C in a power law form

$$S_{22}(t) = \left[1.7051 \ (t)^{0.1954} + 1\right] S_{22}^0 \qquad (19)$$

and

$$S_{66}(t) = \left[11.3076 \ (t)^{0.2771} + 1\right] S_{66}^0, \qquad (20)$$

where

$$S_{22}^0 = 7.5328 \cdot 10^{-7}/\text{psi}$$

$$S_{66}^0 = 1.3834 \cdot 10^{-6}/\text{psi}.$$

The compliance in the fiber direction, $S_{11} = 5.9 \cdot 10^{-8}/\text{psi}$, and Poisson's ratios, $\nu_{12} = \nu_{13} = 0.3$, $\nu_{23} = 0.36$, are assumed to be time independent. Thermal expansion coefficients of the composites in three principal directions are $\alpha_{11} = -0.5 \cdot 10^{-6}/°\text{C}$ and $\alpha_{22} = \alpha_{33} = 40.0 \cdot 10^{-6}/°\text{C}$, where the negative value indicates shrinkage with temperature increase.

Figures 4 and 5 show radial displacement and radial stress profiles across the thickness of the cylinder at three instants, $t = 10^{-3}$ min, $t = 10^{4.5}$ min, and $t = 10^{12}$ min, respectively. The radial tractions and displacements satisfied the continuity conditions at the interfaces of layers at all instants. The "saw" shaped radial stress distribution results from the discontinuity of material properties and various fiber orientations. The radial displacement, $w(t)$, reaches a steady state at $t = 10^{12}$ min due to a long-term creep behavior. The radial displacement of most layers reaches a constant value, except at the innermost and outermost portions of the cylinder. The free traction boundary at the surface of cylinders causes the gradients in the radial displacements. A similar phenomena is also observed in the radial stresses showing a constant level of stress distribution in the inner portion of cylinder away from boundary layers at $t = 10^{12}$ min. This long-term creep characteristic reflects the proposed power law form, (19) and (20), of the creep compliances.
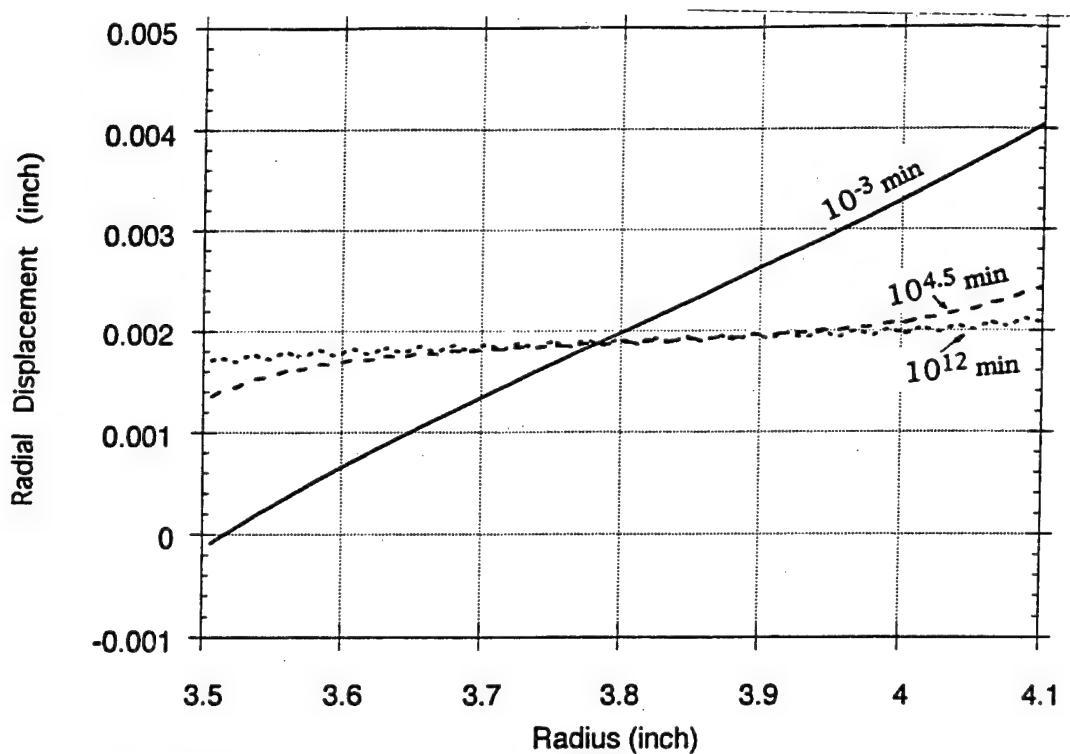
Figure 4. Radial Displacement Profiles Across the Thickness of the Cylinder at Three Different Instants: $t = 10^{-3}$ min, $t = 10^{4.5}$ min, and $t = 10^{12}$ min.
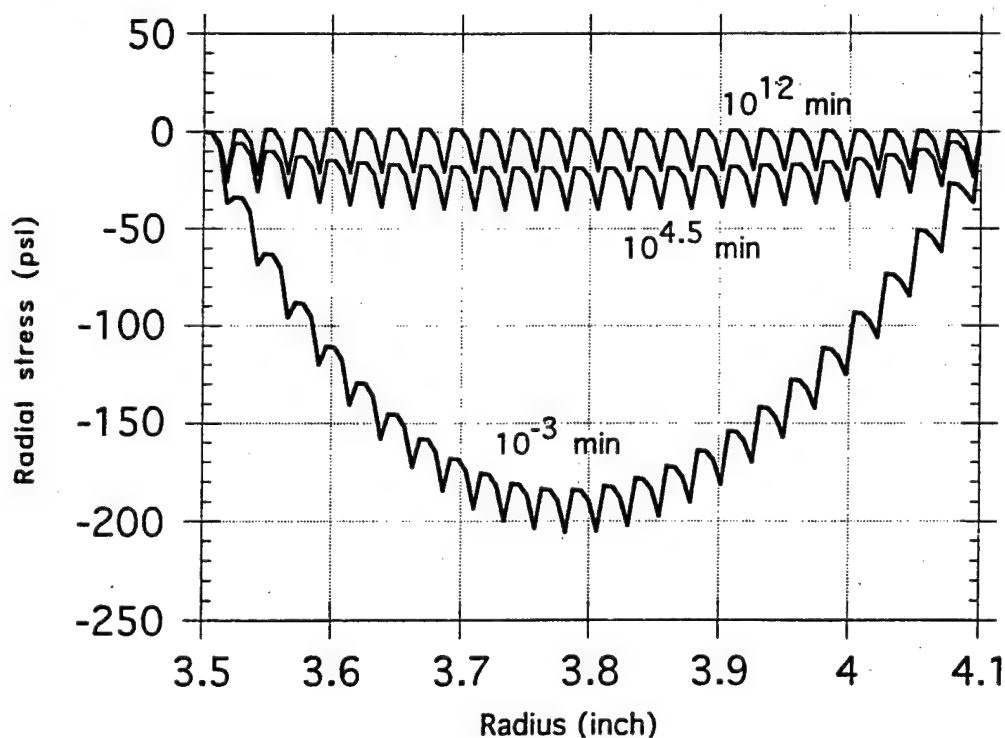

Figure 5. Radial Stress Profiles Across the Thickness of the Cylinder at Three Different Instants: $t = 10^{-3}$ min, $t = 10^{4.5}$ min, and $t = 10^{12}$ min.

11

The hoop stress, $\sigma_{\theta\theta}(t)$ through the thickness of the cylinder, is illustrated at three instants in Figures 6(a), 6(b), and 6(c), respectively. There exist two distinct values (discontinuity) of $\sigma_{\theta\theta}(t)$ across each interface of two adjacent layers due to the various fiber orientations through the thickness. There is a trend showing the creep behavior of the hoop stress profiles from $t = 10^{-3}$ min to $t = 10^{12}$ min. The hoop stresses in 60° and 90° layers show a fairly steep gradient across the cylinder thickness initially. However, the gradient gradually disappears as time approaches infinity. Likewise, Figures 7(a), 7(b), and 7(c) present the axial stress $\sigma_{zz}(t)$ profiles in the radial direction at the three specified instants, respectively. These figures exhibit similar creep and stress relaxation behaviors as those of hoop stresses $\sigma_{\theta\theta}(t)$. However, the axial stresses in 30° and 60° layers show an increase outwardly from the inside of the cylinder in the early stage. Figures 8(a), 8(b), and 8(c) are the inplane shear stresses $\sigma_{z\theta}(t)$ through the thickness of the cylinder at the three specified instants, respectively. The inplane shear stresses of 0° and 90° layers vanish in the entire time history due to generalized plane strain assumption. A drastic change occurs in the 30° and 60° layers, resulting from the combined effects of Poisson's ratio and creep characteristics of materials.

4. Relaxation of Mechanical Stresses

In the following study, a calculation was performed to simulate a composite cylinder pressed fit on a rigid steel mandrel as shown in a schematic in Figure 9. The 0.6-in-thick composite cylinder has a layup construction of $[90/90/90/0]_{25}$, 75% in hoop and 25% in axial direction. The contact pressure is 1,000 psi at the interface of composite and mandrel, which results from the initial interference. The assembly is then heated and held at 93° C constantly for creep study. In modeling of the experiment, the inner radius of the composite overwrap was held constantly to allow creep and stress relaxation of the cylinder occurring at 93° C. The AS-4/epoxy composite material properties were obtained from Kim and Hartness (1987). A power equation was obtained by a least-square curve-fit technique as follows (Tzeng 1997):

$$S_{22}(t) = 7.553 * 10^{-7} (t)^{0.0175} \tag{21}$$

and

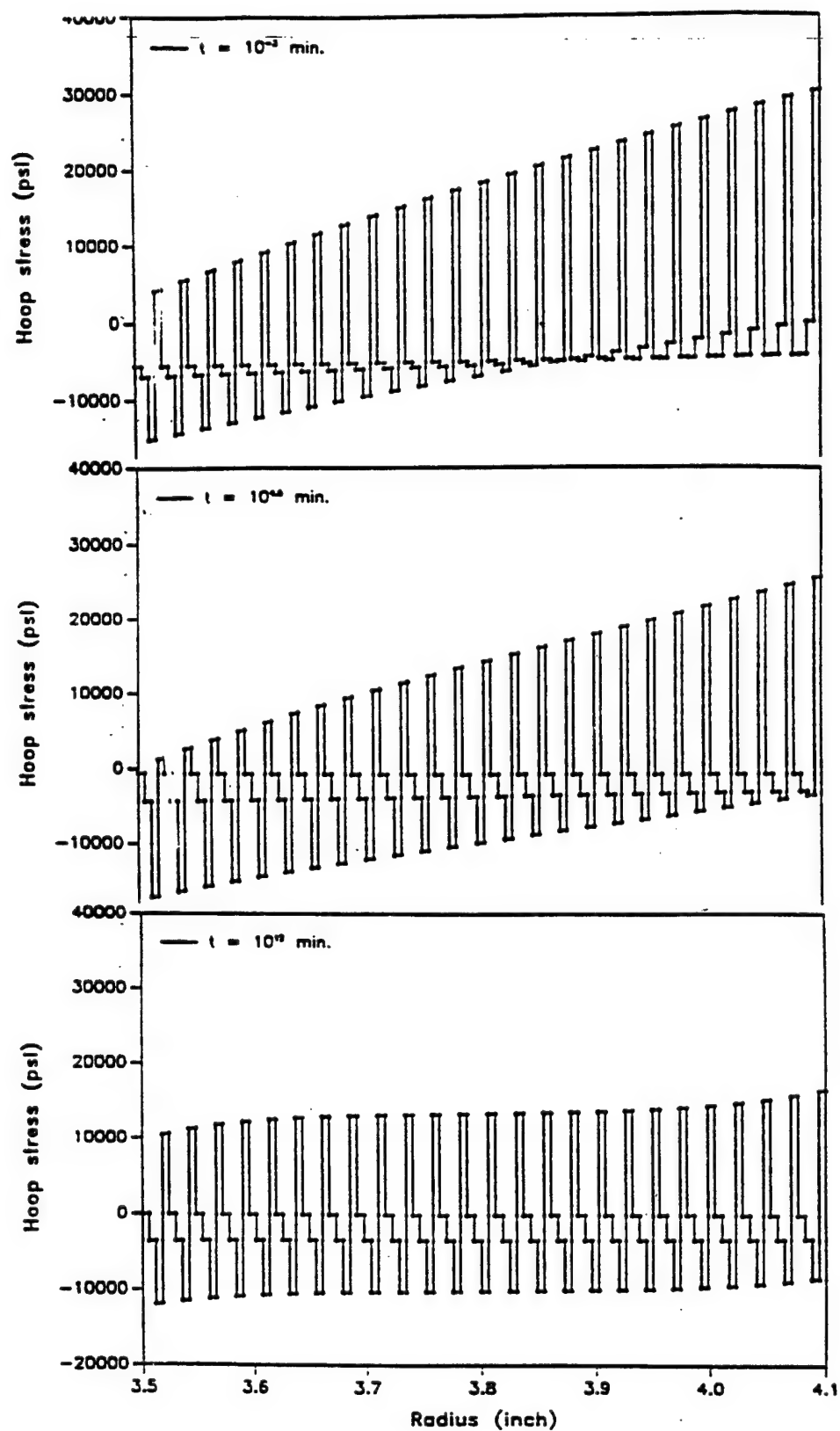$$S_{66}(t) = 1.383 * 10^{-6} (t)^{0.06}. \tag{22}$$

12

Figure 6. Hoop Stress Profiles Across the Thickness of the Cylinder at Three Different Instants: (a) $t = 10^{-3}$ min, (b) $t = 10^{4.5}$ min, and (c) $t = 10^{12}$ min.
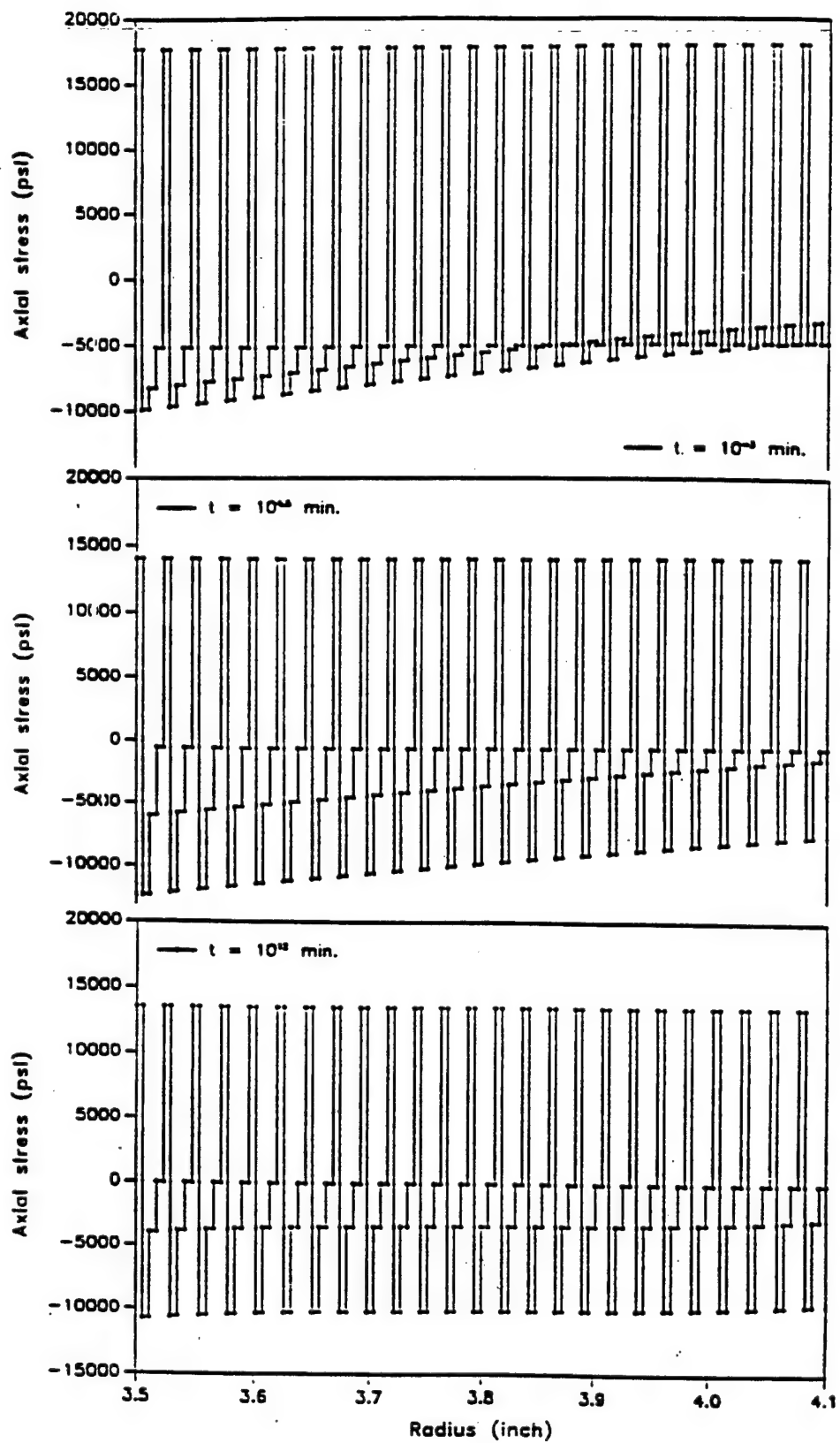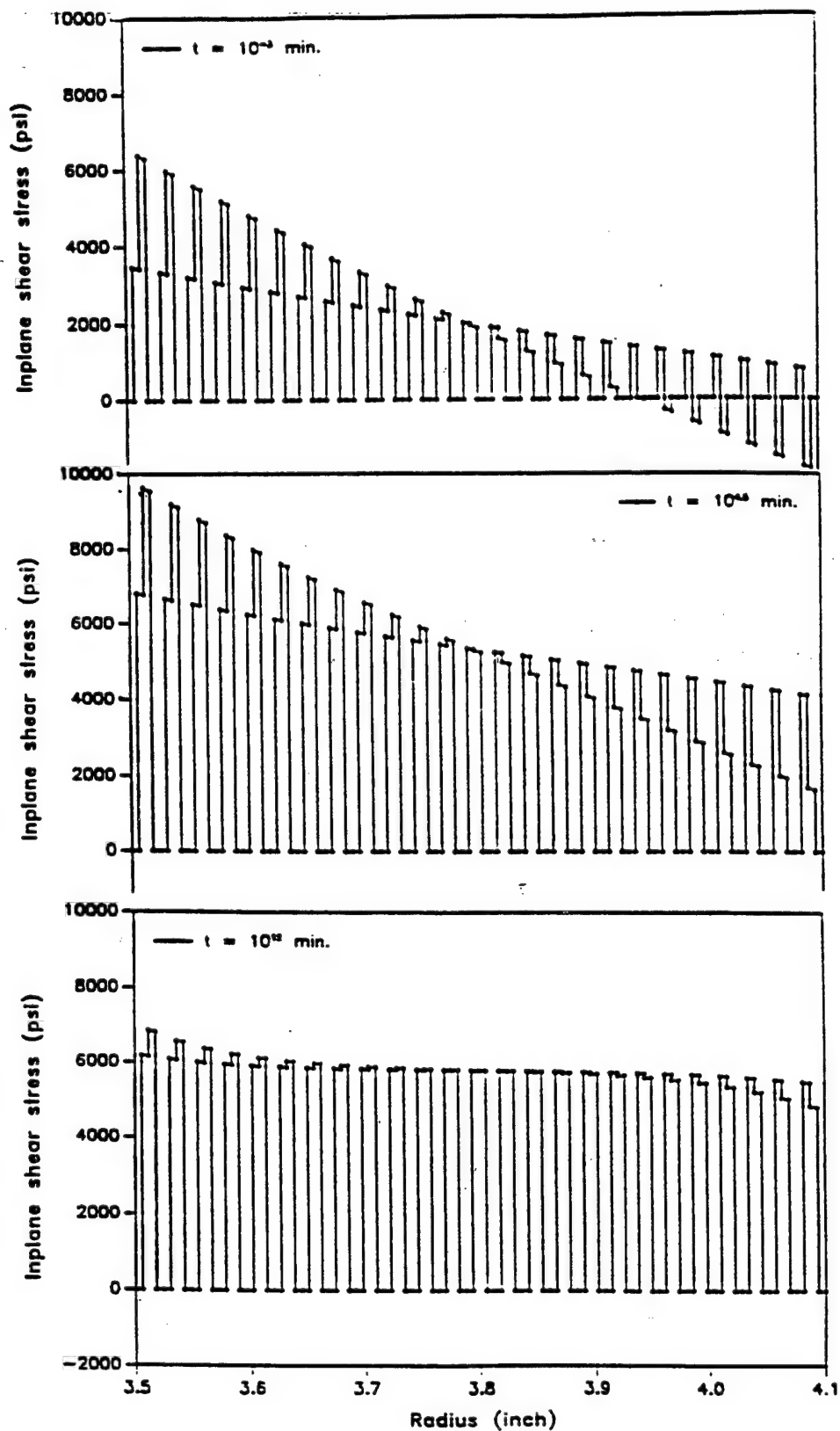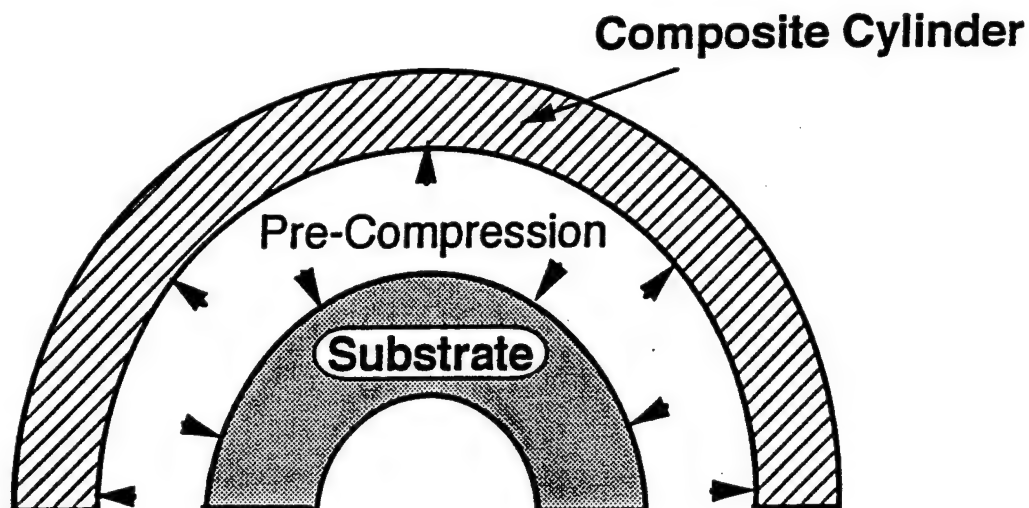
13

Figure 7. Axial Stress Profiles Across the Thickness of the Cylinder at Three Different Instants: (a) $t = 10^{-3}$ min, (b) $t = 10^{4.5}$ min, and (c) $t = 10^{12}$ min.

14

Figure 8. Inplane Shear Stress Profiles Across the Thickness of the Cylinder at Three Different Instants: (a) t = 10⁻³ min, (b) t = 10⁴·⁵ min, and (c) t = 10¹² min.

Figure 9. Precompression at the Interface of a Composite Cylinder and Rigid Mandrel Can Be Achieved By a Press-Fit Process With a Proper Interference.

The transverse and shear compliances are in a unit of 1/psi. The compliance in the fiber direction is also assumed to be elastic, as discussed in the previous section.

Figures 10 and 11 illustrate the creep behavior of radial displacement and relaxation of radial stresses as a function of time, respectively. As shown in the plots, a significant loss of preload was in the composite cylinder constructed with this specific material and layup, subjected to an elevated temperature. Tests have been performed using similar basis graphite/epoxy composite materials, and about 20% of preload was lost in a few weeks at elevated temperatures. In general, the rate of loss of preload increases as the temperature increases. The stress relaxation in hoop-wound fiber layers results mainly from Poisson's effects of creep in the transverse direction since the properties are assumed to be elastic in the fiber direction. The stresses will not
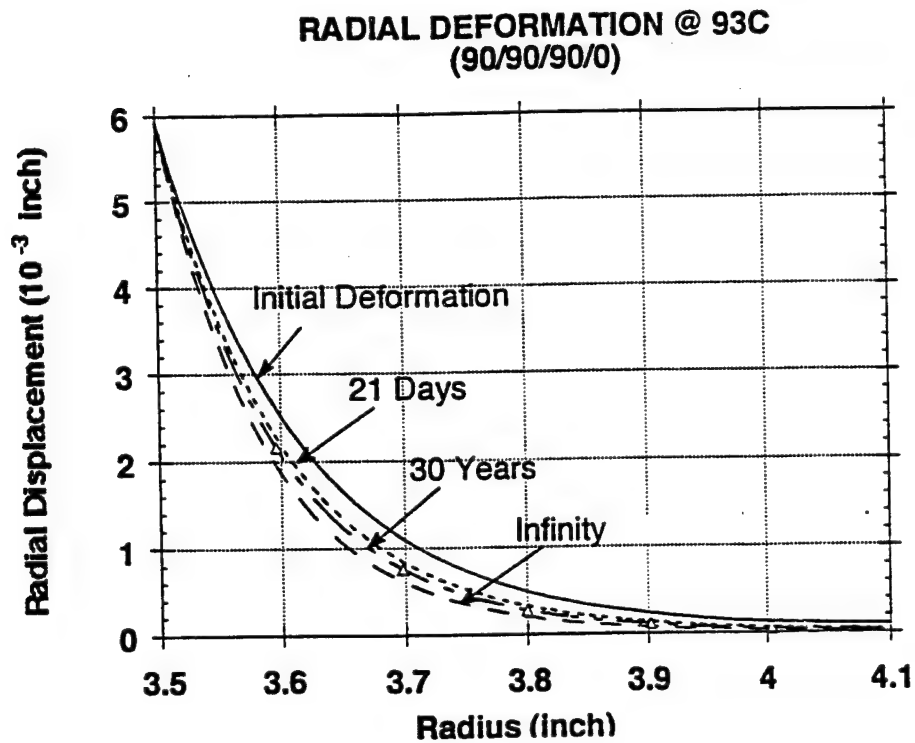
16

RADIAL DEFORMATION @ 93C
(90/90/90/0)

Figure 10. Creeping With Time of the Radial Displacement Through the Thickness of a Composite Overwrapped Cylinder.

DECREASE OF PRE-LOAD @ 93 C
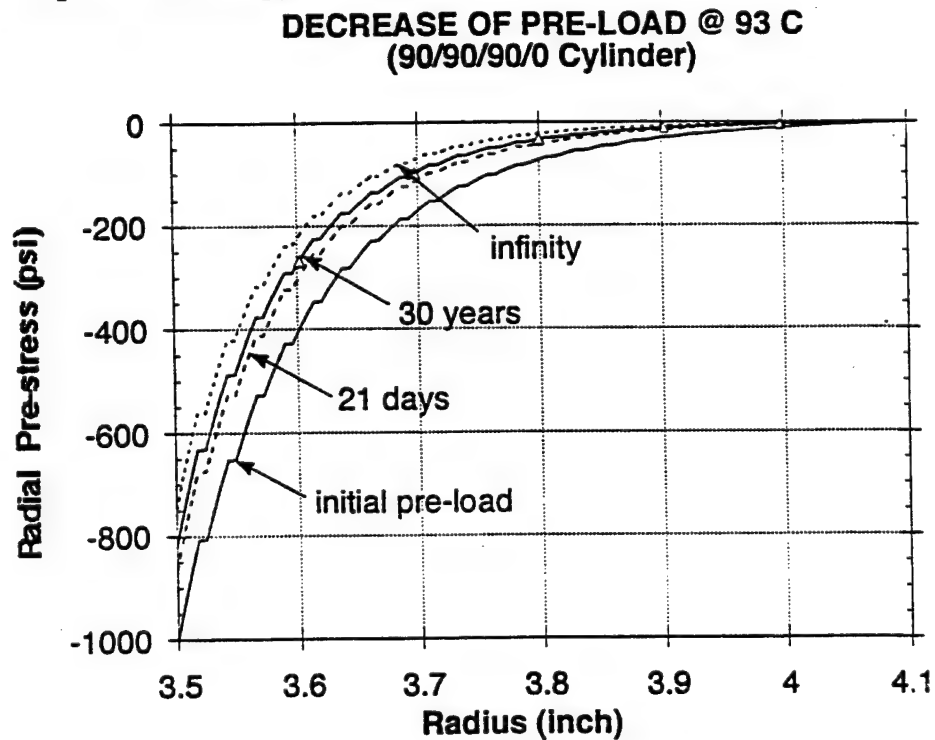**(90/90/90/0 Cylinder)**

Figure 11. Relaxation With Time of Radial Stress Through the Thickness of a Composite Overwrapped Cylinder.

17

diminish completely due to elastic properties in the fiber direction. However, the reduction and redistribution of hoop stresses will cause a decrease of the radial compression in the cylinders in a long period. As the radial displacement approaches a uniform state through the thickness, the radial stress will diminish completely, depending upon the material properties and temperatures.

The viscoelastic properties are commonly not available for most composite materials. There is a need to develop a simple and accurate estimation of the viscoelastic properties of composite material for the analysis. This is especially important from an application point of view since there are numerous composite systems available through a combination of matrix and fiber. The following approach is proposed to provide a proper method of material selection based on creep and stress relaxation consideration. The creep compliance of matrix alone can be measured using dynamic mechanical analysis (DMA). Figure 12 shows the measured data of ICI/Fibrite 977-2 resin at a reference temperature of 121° C. The data can then be curve-fit with a time-dependent function as follows:

$$S(t) = S_o \times (t)^{0.04} \tag{23}$$

The expression basically represents the time dependency of the matrix material of composite material. Since the viscoelastic behavior of composite material is mainly dominated by the matrix, it is reasonable to assume the transverse and shear properties of graphite/epoxy (977-2 resin) composite following the power law as equation (23). The elastic properties that are generally available can then be substituted into the expression as the term "S_o" to obtain the viscoelastic properties for the specific composite system. The proposed approach can significantly reduce engineering efforts in material testing if the approximated properties can be applied to the viscoelastic analysis resulting in good agreement with experiment.

In the following study, a cylinder analysis was performed and compared to experimental data. A cylinder with an inner diameter of 10.0 in and a thickness of 1.2 in was fabricated from graphite/epoxy (Im7/977-2) composite material. The laminated cylinder has a ply construction of
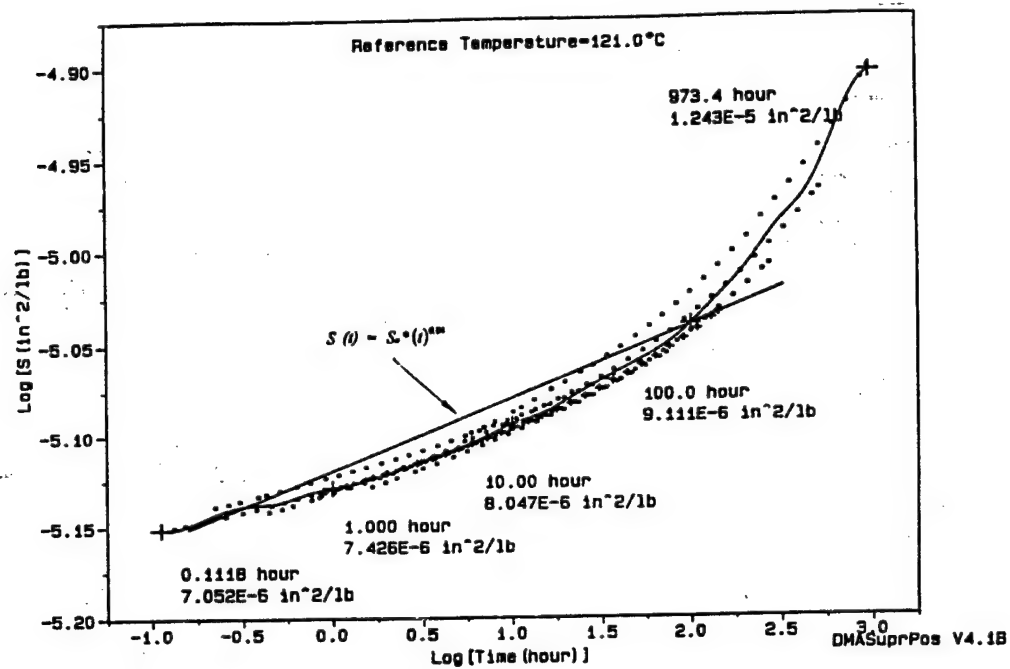
18

Figure 12. Creep Compliance of Fibrite 977-2 Epoxy Measured by DMA at a Reference Temperature of 121° C (Raw Data Are Provided by CEM, University of Texas at Austin).
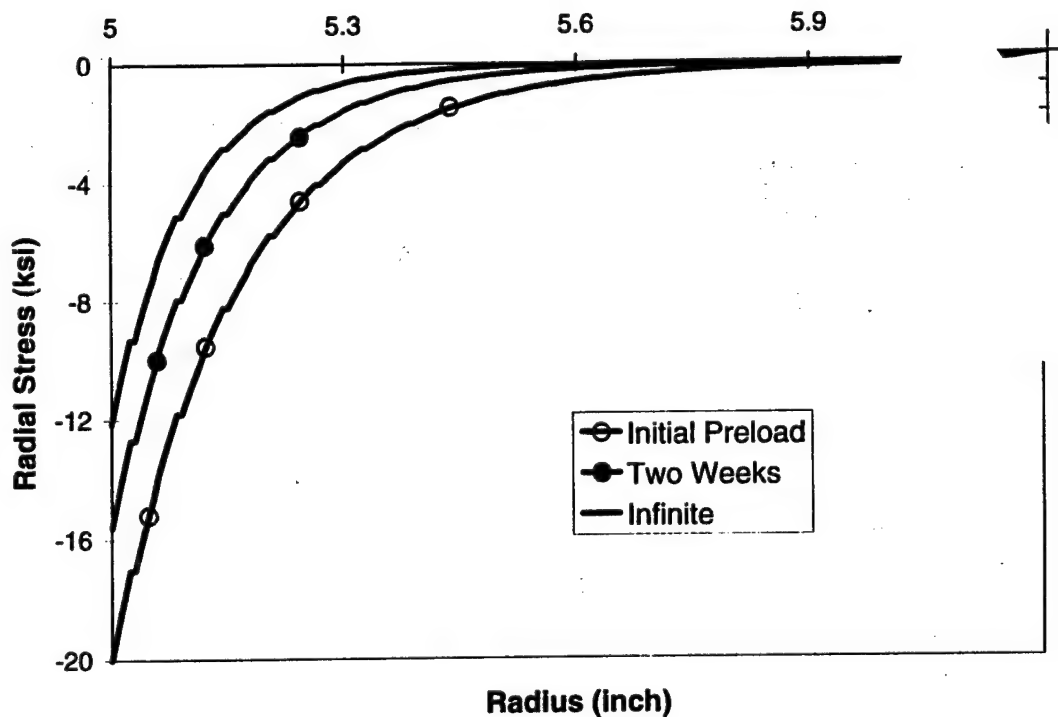

Figure 13. Relaxation of Interference Pressure of a 10-in-Diameter Composite Cylinder at Three Time Instants.

an interference pressure of 20 ksi. The entire assembly is then kept in an oven at 121° C. The hoop strain at the inner radius of the mandrel is monitored, which provides a measure of the preload variation. A loss of preload was found to be 18% in about 14 days. The result of analysis is shown in Figure 13, which indicates a fairly good agreement. Although the validation is limited to a single experiment so far, the correlation does provide confidence of implementation of the proposed approach.

5. Conclusions

An analysis has been developed to study the thermal viscoelastic behavior of thick-walled laminated composite cylinders with ply-by-ply variation of anisotropic viscoelastic properties. The relaxation of stresses and creep behaviors is properly determined in a cylinder subjected to a uniform temperature change. The extreme anisotropy of the viscoelastic behavior of composites results in very interesting as well as important long-term characteristics of cylinders, which cannot be modeled using currently available finite-element codes. Creep and stress relaxation exists in the fiber direction even though the fiber-dominant properties are elastic. This is mainly due to the contribution of the Poisson's effects of viscoelastic transverse and shear properties. Furthermore, the analysis is extended to study the viscoelastic behavior of composite overwrapped cylinders with built-in mechanical preloads. The relaxation of preload in the composite is critical to the service life cycle of applications such as gun tubes and composite rotors, which are designed and built with a preload to achieve desired mechanical performance.

6. References

Chien, L. S., and J. T. Tzeng. "A Thermal Viscoelastic Analysis for Thick-Walled Composite Cylinders." *Journal of Composite Materials,* vol. 29, no. 4, pp. 525–548, 1995.

Christensen, R. M. *Theory of Viscoelasticity, An Introduction, 2nd edition.* New York: Academic Press, Inc., 1982.

Ferry, J. D. *Viscoelastic Properties of Polymer.* New York: John Wiley & Sons, Inc., 1961.

Hashin, Z. "Viscoelastic Behavior of Heterogeneous Media." *Journal of Applied Mechanics,* vol. 32, pp. 630–636, 1965.

Kim, R. Y., and J. T. Hartness. "Time-Dependent Response of AS-4/PEEK Composite." *Proceedings of the 19th International SAMPE Technical Conference*, pp. 468–475, October 1987.

Muki, R., and E. Sternberg. "On Transient Thermal Stresses in Viscoelastic Materials With Temperature-Dependent Properties." *Journal of Applied Mechanics,* pp. 193–207, 1961.

Rogers, T. G., and E. H. Lee. "The Cylinder Problem in Viscoelastic Stress Analysis." *Quarterly of Applied Mathematics,* vol. 22, pp. 117–131, 1964.

Schapery, R. A. "Application of Thermodynamics to Thermomechanical, Fracture, and Birefringent Phenomena in Viscoelastic Media." *Journal of Applied Physics,* vol. 35, no. 5, pp. 1451–1465, 1964.

Schapery, R. A. "Stress Analysis of Viscoelastic Composite Materials." *Journal of Composite Materials,* vol. 1, pp. 228–267, 1967.

Tzeng, J. T. "Viscoelastic Behavior of Composite Rotors at Elevated Temperatures." *IEEE Transactions of Magnetics,* vol. 33, no. 1, pp. 413–418, 1997.

Tzeng, J. T., and L. S. Chien. "A Thermal/Mechanical Model of Axially Loaded Thick-Walled Composite Cylinders." *Journal of Composites Engineering,* vol. 4, no. 2, pp. 219–232, 1994.

Williams, M. L. "Structural Analysis of Viscoelastic Materials." *AIAA Journal,* vol. 2, no. 5, pp. 785–808, 1964.

INTENTIONALLY LEFT BLANK.

2   DEFENSE TECHNICAL
    INFORMATION CENTER
    DTIC DDA
    8725 JOHN J KINGMAN RD
    STE 0944
    FT BELVOIR VA 22060-6218

1   HQDA
    DAMO FDQ
    DENNIS SCHMIDT
    400 ARMY PENTAGON
    WASHINGTON DC 20310-0460

1   DPTY ASSIST SCY FOR R&T
    SARD TT F MILTON
    RM 3EA79 THE PENTAGON
    WASHINGTON DC 20310-0103

1   OSD
    OUSD(A&T)/ODDDR&E(R)
    J LUPO
    THE PENTAGON
    WASHINGTON DC 20301-7100

1   CECOM
    SP & TRRSTRL COMMCTN DIV
    AMSEL RD ST MC M
    H SOICHER
    FT MONMOUTH NJ 07703-5203

1   PRIN DPTY FOR TCHNLGY HQ
    US ARMY MATCOM
    AMCDCG T
    M FISETTE
    5001 EISENHOWER AVE
    ALEXANDRIA VA 22333-0001

1   PRIN DPTY FOR ACQUSTN HQS
    US ARMY MATCOM
    AMCDCG A
    D ADAMS
    5001 EISENHOWER AVE
    ALEXANDRIA VA 22333-0001

1   DPTY CG FOR RDE HQS
    US ARMY MATCOM
    AMCRD
    BG BEAUCHAMP
    5001 EISENHOWER AVE
    ALEXANDRIA VA 22333-0001

1   INST FOR ADVNCD TCHNLGY
    THE UNIV OF TEXAS AT AUSTIN
    PO BOX 202797
    AUSTIN TX 78720-2797

1   USAASA
    MOAS AI W PARRON
    9325 GUNSTON RD STE N319
    FT BELVOIR VA 22060-5582

1   CECOM
    PM GPS COL S YOUNG
    FT MONMOUTH NJ 07703

1   GPS JOINT PROG OFC DIR
    COL J CLAY
    2435 VELA WAY STE 1613
    LOS ANGELES AFB CA 90245-5500

1   ELECTRONIC SYS DIV DIR
    CECOM RDEC
    J NIEMELA
    FT MONMOUTH NJ 07703

3   DARPA
    L STOTTS
    J PENNELLA
    B KASPAR
    3701 N FAIRFAX DR
    ARLINGTON VA 22203-1714

1   USAF SMC/CED
    DMA/JPO
    M ISON
    2435 VELA WAY STE 1613
    LOS ANGELES AFB CA
    90245-5500

1   US MILITARY ACADEMY
    MATH SCI CTR OF EXCELLENCE
    DEPT OF MATHEMATICAL SCI
    MDN A MAJ DON ENGEN
    THAYER HALL
    WEST POINT NY 10996-1786

1   DIRECTOR
    US ARMY RESEARCH LAB
    AMSRL CS AL TP
    2800 POWDER MILL RD
    ADELPHI MD 20783-1145

3   CDR US ARMY ARDEC
AMSTA AR TD
V LINDNER
T PRICE
C SPINELLI
PICATINNY ARSENAL NJ
07806-5000

1   CDR USA BELVOIR RD&E CTR
STRBE JBC
FORT BELVOIR VA 2200-5605

4   CDR US ARMY MICOM
AMSMI RD W MCCORKLE
AMSMI RD ST P DOYLE
AMSMI RD ST CN T VANDIVER
AMSMI RD ST WF M COLE
REDSTONE ARSENAL AL 35898

3   CDR WATERVLIET ARS
SMCWV QAE Q C HOWD
SMCWV QA QS K INSCO
SMCWV SPM T MCCLOSKEY
B25 3
WATERVLIET NY 12189-4050

4   DIR ARO
G ANDERSON
J CHANDRA
A CROWSON
R SINGLETON
PO BOX 12211
RESEARCH TRIANGLE PARK NC
27709-2211

9   DIR BENET LABS
AMSTA AR CCB
C KITCHENS
J KEANE
J BATTAGLIA
J VASILAKIS
G FRIAR
V MONTVORI
J WRZOCHALSKI
R HASENBEIN
AMSTA AR CCB R S SOPOK
WATERVLIET NY 12189-4050

1   DIR USA CRREL
P DUTTA
72 LYME RD
HANOVER NH 03755

2   DIR DARPA
J KELLY
B WILCOX
3701 N FAIRFAX DR
ARLINGTON VA 22203-1714

1   EXPDTNRY WF DIV N85
F SHOUP
2000 NAVY PENTAGON
WASHINGTON DC 20350-2000

2   OFC OF NAVAL RSCH
MECH DIV CODE 1132SM
Y RAJAPAKSE
D SIEGEL 351
800 N QUINCY ST
ARLINGTON VA 22217

1   DAVID TAYLOR RSCH CTR
SHIP STRCTRS & PRTCTN DEPT
J CORRADO CODE 1702
BETHESDA MD 20084

2   DAVID TAYLOR RSCH CTR
R ROCKWELL
W PHYILLAIER
BETHESDA MD 20054-5000

1   NAVAL ORD STN
ADVNCD SYS TECH BR
D HOLMES CODE 2011
LOUISVILLE KY 40214-5245

1   CDR NSSC
D LIESE
2531 JEFFERSON DVS HWY
ARLINGTON VA 22242-5160

5   CDR NSWC
CODE D4 M E LACY
CODE G30 J H FRANCIS
CODE G33 J FRAYSSE
G GRAFF
R HUBBARD 3 CP
DAHLGREN VA 22448

28

3	ALLIANT TECHSYS INC J BODE C CANDLAND K WARD 5901 LINCOLN DR MINNEAPOLIS MN 55346-1674
1	ALLIANT TECHSYS INC T HOLMQUIST 600 SECOND ST NE HOPKINS MN 55343
1	AMOCO PRFRMNC PRODUCTS M MICHNO JR 4500 MCGINNIS FERRY RD ALPHARETTA GA 30202-3944
1	APPLIED COMPOSITES W GRISCH 333 NO SIXTH ST ST CHARLES IL 60174
1	BRUNSWICK DFNS T HARRIS 174 JFRSN DVS HWY STE 410 ARLINGTON VA 22202
1	CHAMBERLAIN MFG CORP R&D DIV M TOWNSEND 550 ESTHER ST WATERLOO IA 50704
1	CSTM ANLYTCL ENGRNG SYS INC A ALEXANDER STAR RT BOX 4A FLINTSTONE MD 21530
3	HERCULES INC R BOE J POESCH F POLICELLI PO BOX 98 MAGNA UT 84044

3	HERCULES INC G KUEBELER B MANDERVILLE JR J VERMEYCHUK HERCULES PLZ WILMINGTON DE 19894
1	HEXCEL M SHELENDICH 11555 DUBLIN BLVD PO BOX 2312 DUBLIN CA 94568-0705
1	IAP RSCH INC A CHALLITA 2763 CULVER AVE DAYTON OH 45429
1	INTGRTD CMPST TECH H PERKINSON JR PO BOX 397 YORK NEW SALEM PA 17371-0397
1	INTERFEROMETRICS INC R LARRIVA VP 8150 LESSBURG PIKE VIENNA VA 22100
1	KAMAN SCNCS CORP T HAYDEN PO BOX 7463 COLORADO SPRINGS CO 80933
2	LORAL VOUGHT SYS K COOK G JACKSON 1701 W MARSHALL DR GRAND PRAIRIE TX 75051
2	MARTIN MARIETTA CORP P DEWAR L SPONAR 230 E GODDARD BLVD KING OF PRUSSIA PA 19406
1	NOESIS INC A BOUTZ 1500 WILSON BLVD STE 1224 ARLINGTON VA 22209

2   PRIMEX TECH
       FLNCHBGH DIV
       E STEINER
       B STEWARD
       PO BOX 127
       RED LION PA 17356

1   PRIMEX TECH
       L WHITMORE
       10101 9TH ST NO
       ST PETERSBURG FL 33702

ABERDEEN PROVING GROUND

27   DIR USARL
       AMSRL WM,
            L JOHNSON
            J MCCAULEY
            D VIECHNICKI
            G HAGNAUER
       AMSRL WM P,
            A HORST
            E SCHMIDT
       AMSRL WM PB, P PLOSTINS
       AMSRL WM MB,
            J BENDER
            L BURTON
            B BURNS
            W DRYSDALE
            D GRANVILLE
            D HOPKINS
            D HENRY
            C HOPPEL
            R KASTE
            J TZENG
            A FRYDMAN
            B FINKS
            T BOGETTI
       AMSRL WM T, W F MORRISON
       AMSRL WM TA,
            W BRUCHEY
            W GILLICH
       AMSRL WM TC,
            R COATES
            W DE ROSSET
       AMSRL WM WA, B MOORE
       AMSRL WM WC , T HAUG

REPORT DOCUMENTATION PAGE

Public reporting burden for this collection of information is estimated to average 1 hour per response, including the time for reviewing instructions, searching existing data sources, gathering and maintaining the data needed, and completing and reviewing the collection of information. Send comments regarding this burden estimate or any other aspect of this collection of information, including suggestions for reducing this burden, to Washington Headquarters Services, Directorate for Information Operations and Reports, 1215 Jefferson Davis Highway, Suite 1204, Arlington, VA 22202-4302, and to the Office of Management and Budget, Paperwork Reduction Project(0704-0188), Washington, DC 20503.

1. AGENCY USE ONLY (Leave blank)	2. REPORT DATE	3. REPORT TYPE AND DATES COVERED
	January 1998	Final, Oct 95 - Dec 96

4. TITLE AND SUBTITLE	5. FUNDING NUMBERS
Viscoelastic Response of Prestressed Composite Cylinders for Rotating Machinery Applications	PR: 1L162618AH80

6. AUTHOR(S)

Jerome T. Tzeng

7. PERFORMING ORGANIZATION NAME(S) AND ADDRESS(ES)	8. PERFORMING ORGANIZATION REPORT NUMBER
U.S. Army Research Laboratory ATTN: AMSRL-WM-MB Aberdeen Proving Ground, MD 21005-5066	ARL-TR-1590

9. SPONSORING/MONITORING AGENCY NAMES(S) AND ADDRESS(ES)	10. SPONSORING/MONITORING AGENCY REPORT NUMBER

11. SUPPLEMENTARY NOTES

12a. DISTRIBUTION/AVAILABILITY STATEMENT	12b. DISTRIBUTION CODE
Approved for public release; distribution is unlimited.	

13. ABSTRACT (Maximum 200 words)

Energy storage devices such as composite rotors are built with radial precompression to enhance mechanical performance; however, the preload might decrease due to the viscoelastic behavior of materials at elevated temperatures. In this investigation, an analytical solution is developed to study the viscoelastic problem of thick-walled cylinders. The analysis accounts for ply-by-ply variations of properties, fiber orientations, and temperature gradients through the thickness of cylinders. Fiber-reinforced composite materials generally illustrate extreme anisotropy in viscoelastic behavior. The viscoelasticity exists mainly in matrix-dominant properties such as transverse and shear while the fiber-dominant properties behave more like elastic mediums. Accordingly, the viscoelastic characteristics of composite cylinders are quite different from those of isotropic cylinders. Currently, finite-element packages such as ABAQUS, ANSYS, and DYNA3D are not suitable for the viscoelastic analysis of composite cylinders because of the lack of anisotropic viscoelastic elements. The prestress in the hoop-wound fibers, which generates radial compression in the cylinders, might decrease due to Poisson's effect alone from the creep behavior in the transverse properties of composite. The result also shows the effects of layup construction and fiber orientations on the anisotropic behavior of composite cylinders.

14. SUBJECT TERMS			15. NUMBER OF PAGES
composite, viscoelasticity, compulsator			35
			16. PRICE CODE

17. SECURITY CLASSIFICATION OF REPORT	18. SECURITY CLASSIFICATION OF THIS PAGE	19. SECURITY CLASSIFICATION OF ABSTRACT	20. LIMITATION OF ABSTRACT
UNCLASSIFIED	UNCLASSIFIED	UNCLASSIFIED	UL

NSN 7540-01-280-5500

INTENTIONALLY LEFT BLANK.

USER EVALUATION SHEET/CHANGE OF ADDRESS

This Laboratory undertakes a continuing effort to improve the quality of the reports it publishes. Your comments/answers to the items/questions below will aid us in our efforts.

1. ARL Report Number/Author __ARL-TR-1590 (Tzeng)_____ Date of Report __January 1998_____

2. Date Report Received _____

3. Does this report satisfy a need? (Comment on purpose, related project, or other area of interest for which the report will be used.) _____

_____

_____

4. Specifically, how is the report being used? (Information source, design data, procedure, source of ideas, etc.) _____

_____

_____

5. Has the information in this report led to any quantitative savings as far as man-hours or dollars saved, operating costs avoided, or efficiencies achieved, etc? If so, please elaborate. _____

_____

_____

6. General Comments. What do you think should be changed to improve future reports? (Indicate changes to organization, technical content, format, etc.) _____

_____

_____

_____

CURRENT
ADDRESS

_____

Organization

_____

Name   E-mail Name

_____

Street or P.O. Box No.

_____

City, State, Zip Code

7. If indicating a Change of Address or Address Correction, please provide the Current or Correct address above and the Old or Incorrect address below.

OLD
ADDRESS

_____

Organization

_____

Name

_____

Street or P.O. Box No.

_____

City, State, Zip Code

(Remove this sheet, fold as indicated, tape closed, and mail.)
(DO NOT STAPLE)